Activation of Phospholipase C Increases Intramembrane Electric Fields in N1E-115 Neuroblastoma Cells

Chang Xu and Leslie M. Loew
Department of Physiology and Center for Biomedical Imaging Technology, University of Connecticut Health Center, Farmington, Connecticut 06030

ABSTRACT We imaged the intramembrane potential (a combination of transmembrane, surface, and dipole potential) on N1E-115 neuroblastoma cells with a voltage-sensitive dye. After activation of the B_2 bradykinin receptor, the electric field sensed by the dye increased by an amount equivalent to a depolarization of 83 mV. The increase in intramembrane potential was blocked by the phospholipase C (PLC) inhibitors U-73122 and neomycin, and was invariably accompanied by a transient rise of $[Ca^{2+}]_i$. A depolarized inner surface potential, as the membrane loses negative charges via phosphatidylinositol 4,5-bisphosphate (PIP_2) hydrolysis, and an increase in the dipole potential, as PIP_2 is hydrolyzed to 1,2-diacylglycerol (DAG), can each account for a small portion of the change in intramembrane potential. The primary contribution to the measured change in intramembrane potential may arise from an increased dipole potential, as DAG molecules are generated from hydrolysis of other phospholipids. We found bradykinin produced an inhibition of a M-type voltage-dependent K^+ current ($I_{K(M)}$). This inhibition was also blocked by the PLC inhibitors and had similar kinetics as the bradykinin-induced modulation of intramembrane potential. Our results suggest that the change in the local intramembrane potential induced by bradykinin may play a role in mediating the $I_{K(M)}$ inhibition.

INTRODUCTION

Although the behavior of the voltage-gated ion channels in cell membranes is physiologically modulated by the transmembrane potential, the regulatory elements in the channels (e.g., gating charges) are fundamentally responding to the electric field within the plasma membrane—the intramembrane electric field, which is generated by a complicated sum of transmembrane potential, surface potential, and dipole potential (for reviews, see Honig et al., 1986; Loew, 1993). Surface potential is the electric potential difference between the membrane-aqueous interface and the bulk aqueous solutions (for reviews, see McLaughlin, 1977, 1989). The difference between the negative surface potential on the outer and inner surfaces of a cell membrane contributes to the intramembrane electric field. Cell membranes also possess a substantial dipole potential arising from the oriented dipoles of lipid ester groups or immobilized water molecules at the membrane-water interface (Szabo, 1974, 1977; Clarke, 1997; Flewelling and Hubbell, 1986; Franklin and Cafiso, 1993; Gawrisch et al., 1992; Zheng and Vanderkooi, 1992). This potential is on the order of several hundred mVs, positive in the interior of the membrane. Like transmembrane potential, membrane surface potential (Chandler et al., 1965; Gilbert and Ehrenstein, 1969; McLaughlin, 1989) can modulate the activity of voltage-dependent ion channels by changing the intramembrane electric field. The effect of dipole potential on ion channel activity is less well studied. However, there is evidence indicating that modulators of dipole potential such as phloretin and cholesterol do affect the potassium current in the squid giant axon (Strichartz et al., 1980) and voltage-dependent calcium channels in several cell types (Locher et al., 1984; Zhou et al., 1991; Sen et al., 1992). In differentiated N1E-115 cells, it has been found in this lab that the voltage-gated sodium channels of the growth cone have a faster activation rate than those in the soma (Zhang et al., 1996), possibly because the growth cone region has a more positive dipole potential than the soma membrane (Bedlack et al., 1994).

Whether the activation of membrane receptors can modulate intramembrane potential, especially surface potential and dipole potential, has not been investigated, perhaps because appropriate methods for monitoring the intramembrane potential in cells have not been well established. In particular, we are interested in the possible change in intramembrane potential after receptor activation of phospholipase C (PLC). Activation of PLC leads to hydrolysis of phosphatidylinositol 4,5-bisphosphate (PIP_2) to the second messengers, diacylglycerol and inositol 1,4,5-trisphosphate (IP_3) (Berridge, 1993). Whereas IP_3 causes Ca^{2+} release from intracellular Ca^{2+} stores by activating IP_3 receptors, diacylglycerol activates protein kinase C (PKC) thereby modulating a wide range of cellular responses. Recently, it has been suggested that changes in PIP_2 concentration could play an important role in regulating cellular processes (Lee and Rhee, 1995). The anionic PIP_2 comprises 0.1%–5% of total lipids in the inner leaflet of the membrane of most cells (Kleinig, 1970; Tran et al., 1993). We hypothesize that the surface potential and dipole potential profile of the membrane may be changed after hydrolysis of PIP_2 based on the following two findings: first, a decrease in PIP_2 concentration could lead to a change in the surface potential

Submitted May 16, 2002, and accepted for publication February 6, 2003.
Address reprint requests to Leslie M. Loew, Dept. of Physiology and Center for Biomedical Imaging Technology, University of Connecticut Health Center, Farmington, CT 06030. E-mail: les@volt.uchc.edu.

0006-3495/03/06/4144/13 $2.00

(McLaughlin, 1989); secondly, generation of 1,2-diacylglycerol (DAG) from phosphatidylinositol could increase dipole potential, since the dipole potential of a DAG monolayer is 127 mV more positive compared to that of a phosphatidylinositol monolayer (Smaby and Brockman, 1990).

Such intramembrane potentials are impossible to measure using conventional electrodes placed in the bulk solutions, since the surface potentials arising from the negative charges on both surfaces of the plasmalemma decay with a Debye length of under 10 Å in 0.1 M monovalent salt solutions (McLaughlin, 1989; Cevc, 1990; Langner et al., 1990), and the dipole potentials are localized to an ~5 Å thick region within the plasmalemma just below both surfaces (Szabo, 1974, 1977; Clarke, 1997; Flewelling and Hubbell, 1986; Franklin and Cafiso, 1993; Gawrisch et al., 1992; Zheng and Vanderkooi, 1992). However, certain voltage-sensitive dyes can report the local electric field at their location within the membrane. We have shown that the dual wavelength ratio of styryl dyes provides a consistent measure of transmembrane potential (Montana et al., 1989; Zhang et al., 1998). In earlier studies, others and we characterized the ability of di-8-ANEPPS to measure dipole potential changes and variations along the membrane (Bedlack et al., 1994; Cladera and O'Shea, 1998; Clarke, 1997; Clarke and Kane, 1997; Gross et al., 1994). In a recent study (Xu and Loew, 2003), we showed that the styryl dye ratiometric measurements could be used to monitor changes in surface potential.

In this paper, dual wavelength ratiometric imaging of di-8-ANEPPS was used to determine the change in the intramembrane potential of a cell during receptor-mediated activation of the PLC signaling pathway. We used bradykinin (BK) to activate PLC in N1E-115 neuroblastoma cells, a mouse neuroblastoma cell line that expresses a number of G-protein-coupled receptors, including B_2 receptors (Coggan and Thompson, 1995; 1997). BK has also been shown to modulate the M current in these cells, but the mechanism of this modulation remains unclear (Higashida and Brown, 1987). The dye ratio reports a large slow change in intramembrane potential that has the same time course as the modulation of the M current by B_2 receptor activation in these cells. Because $I_{K(M)}$ has been described as a voltage-dependent K^+ current (Constanti and Brown,1981; Brown and Constanti, 1980), this raises the possibility that changes in intramembrane potential may underlie the modulation of $I_{K(M)}$.

METHODS

Cell preparation

N1E-115 mouse neuroblastoma cells were grown and maintained in Dulbecco's modified Eagle's medium containing 10% fetal bovine serum. Cells were grown until 50% confluent before seeding on uncoated glass coverslip. Differentiation was initiated by replacing the media with one containing 0.5% fetal bovine serum and 1% dimethylsulfoxide. Cells were cultured for a further 2–5 days to complete differentiation and achieve neuronal morphology.

Dye loading

For di-8-ANEPPS staining, each coverslip was washed in Eagle's balanced salt solution (EBSS) buffered to pH 7.35 with 20 mM HEPES, and then incubated for 20 min at 4°C in the buffered EBSS supplemented with 1-(3-sulfonatopropyl)-4-[β[2-(di-*n*-octylamino)-6-naphthyl]vinyl]pyridinium betaine (di-8-ANEPPS; 0.5 μM) and Pluronic F-127 (BASF, Wyandotte, MI) (PF-127;0.05%). For double staining with Calcium Green and di-8-ANEPPS, Calcium Green-1-AM (Molecular Probes, Eugene, OR) was diluted to 8 μM in 2 ml EBSS. A single coverslip of cells was immediately added, incubated 30 min at 22–25°C in the dark, and then transferred to fresh EBSS to allow recovery at 37°C for 30 min. The cells were then transferred and incubated in the 4°C buffered EBSS containing di-8-ANEPPS and Pluronic F-127 for another 20 min.

Dual wavelength imaging

Stained cells were mounted on an inverted Zeiss microscope (Axiovert 135 TV) and viewed with an oil objective (Plan-Apochromat 63 × 1.40). Dual wavelength image pairs of di-8-ANEPPS (excitation at 440 and 530 nm, emission >570 nm) were acquired using a cooled CCD camera (Model CH100, Photometrics, Tucson, AZ) on the microscope, controlled by Cellscan Acquisition Control unit (Scanalytics, Marlborough, MA). An additional magnification of ×2.5 was used when fluorescent images were taken. Exposure time was 0.7 s for 440 nm and 1.4 s for 530 nm. A 2 × 2 binning of CCD pixels was used to improve the signal. Autofluorescence signals were negligible at both excitation wavelengths compared with di-8-ANEPPS fluorescence. All experiments were performed at room temperature (22–24°C). For cells that were double labeled for simultaneous calcium and membrane potential imaging, di-8-ANEPPS fluorescence was excited at 440 and 530 nm and detected at >570 nm, whereas Calcium Green fluorescence was excited at 485 nm and detected at 525 nm.

Patch clamp

Micropipettes with tip diameters of 1–2 μm were pulled from glass capillaries (Drummond Scientific 100) using a Model P-80 Brown-Flaming micropipette puller (Sutter Instrument, San Francisco, CA). The resistance of the pipettes was from 3 to 7 MΩ. The patch pipette solution contained (in mM): 80 potassium acetate, 30 KCl, 3 $MgCl_2$, 3 EGTA, 40 HEPES, 1 $CaCl_2$ (PH 7.3 with KOH). The whole-cell patch experiments were performed in N1E-115 neuroblastoma cells with an Axopatch 1D amplifier (Axon Instruments, Foster City, CA). All electrophysiological recordings were performed at room temperature (22–24°C). Whole-cell current clamp was used to monitor membrane potential. We digitized the output signal by using the Clampex program (Axon Instruments).

Lipid vesicles

Solutions were buffered with 20 mM HEPES/Tris, pH 7.0 (21°C), and contained 140 mM NaCl in the absence of any divalent salts. Small unilamellar liposomes were made as described by Deamer and Uster (1983). Briefly, we prepared the lipid vesicles by drying chloroform solutions of either 10 mg egg phosphatidylcholine (PC) (Sigma Chemical, St Louis, MO; type XI-E), or bovine brain phosphatidylserine (PS) (Avanti Polar Lipids, Birmingham, AL), or a mixture of 90% PC and 10% 1-palmitoyl-2-oleoyl-*sn*-glycerol (Avanti Polar Lipids) (PC:DAG), or a mixture of 90% PS and 10% 1-palmitoyl-2-oleoyl-*sn*-glycerol (PS:DAG), under a stream of argon for a minimum of 3 h, resuspending the lipids in 1 ml of the buffer and sonicating to clarity with a Laboratory Supplies (Hicksville, NY) G1128P1T sonifier under an argon atmosphere. For fluorescence measurements, 60 μl

of the vesicle suspension was diluted into 3 ml of buffer containing 0.2 μM di-4-ANEPPS. The corrected excitation spectra of the vesicle suspension were measured with a SPEX CM dual-wavelength fluorescence spectrometer (SPEX Industries, Edison, NJ). All experiments were performed at 21°C.

[^{32}P]PIP$_2$ analysis

To examine the relative PIP_2 content of membrane, N1E-115 cells were grown to 30–40% confluency in 35 mm culture dishes; ~4 × 10^5 cells per culture dish were labeled to equilibrium (48 h) with 25 μCi/ml ^{32}P-PO_4 (carrier free, ICN) at 37° in EBSS. After washing twice to remove the unincorporated ^{32}P, the cells were scraped and suspended with EBSS. Cell lipids were extracted with acidic chloroform-methanol as described previously (Agranoff et al., 1983). An aliquot (20 μl) of the lipid extract was subjected to thin layer chromatography (TLC), using Whatman LK5D plates impregnated with 1% potassium oxalate and 2 mM EDTA, and the mobile phase chloroform-methanol-4 N NH_4OH (45:35:10) (Gonzalez-Sastre and Folch-Pi, 1968). Radioactive bands were identified by cochromatography of a PIP_2 standard. TLC spots were transferred to scintillation vials, suspended in Cytoscint ES (ICN Biomedicals, Aurora, OH), and radioactivity determined by liquid scintillation counting (Packard 2000 CA scintillation counter). A second 20 μl aliquot of the lipid extract was applied to a piece of silica gel scraped from a blank TLC plate with area similar to the scraped PIP_2 spots, and suspended in Cytoscint ES to determine radioactivity of the total lipids spotted.

RESULTS

Bradykinin increases intramembrane potential

The potential gradient inside the membrane (intramembrane potential), which is the sum of contributions from transmembrane potential, dipole potential, and the difference in the surface potentials at both sides of the membrane, was measured with the 440 nm/530 nm fluorescence ratios of di-8-ANEPPS. To calibrate the dye, we first measured the 440 nm/530 nm fluorescence ratios along the plasma membrane of a single cell as a function of the applied transmembrane potential in voltage-clamped N1E-115 neuroblastoma cells as described by Zhang et al. (1998). We found di-8-ANEPPS showed linear dependence of fluorescence ratio on potential with a slope of +13% per 100 mV (data not shown). To monitor the effect of bradykinin on intramembrane potential, we took a pair of fluorescence images every 10 s at the excitation wavelengths of 440 and 530 nm after addition of bradykinin. The correspondent ratios were normalized to the baseline fluorescence ratios taken before the addition of bradykinin to avoid cell-to-cell variation. We expressed the ratio change as a change in intramembrane potential, calculated as: $\Delta V_{IM} = (R - R_0)/R_0 \times 100\%/13\%$, where R is the 440/530 nm fluorescence ratio at different times after bradykinin and R_0 is the baseline fluorescence ratio in the absence of bradykinin. The intramembrane potential, calculated in this way, corresponds to the transmembrane potential change that would be required to produce the observed change in ratio. Note that the dye fundamentally measures the electric field at its site in the membrane. It does not measure a true potential difference between its location and the extracellular ground.

When stimulated with a saturating concentration of bradykinin (1 μM), N1E-115 neuroblastomas showed a highly reproducible change in the fluorescence ratio of di-8-ANEPPS, which was characterized by an increase that returned to baseline even in the continued presence of bradykinin; the average peak increase in the ratio was 10.9 ± 0.5% with a time to peak of 158.2 ± 4.4 s ($n = 11$) (Fig. 1). If this ratio change were solely due to a change in transmembrane potential, it would be equivalent to a depolarization of 83.5 ± 4.0 mV. During our recording period, no apparent phototoxicity was observed, and there was no significant change in fluorescence ratio in the EBSS control group across time ($P > 0.05$, $n = 5$; Fig. 1). Fig. 2 shows a typical recording of changes in intramembrane potential induced by bradykinin on an individual cell. Consistent with earlier studies (Zhang et al., 1998), we can see that the intramembrane electric field is heterogeneous along the cell surface; in Fig. 2, for example, a persistently higher than average ratio can be found in the membrane patch centered at 3 o'clock. Comparison between the changes in intramembrane potential along the whole cell and along the high ratio area reveals no significant difference (Fig. 2, *B* and *C*).

Bradykinin inhibits M current and depolarizes the membrane

The change in intramembrane electric field may arise from changes in transmembrane potentials, surface potentials, and dipole potentials. Bradykinin has been reported to be able to inhibit $I_{K(M)}$ (Higashida and Brown, 1987) and depolarize

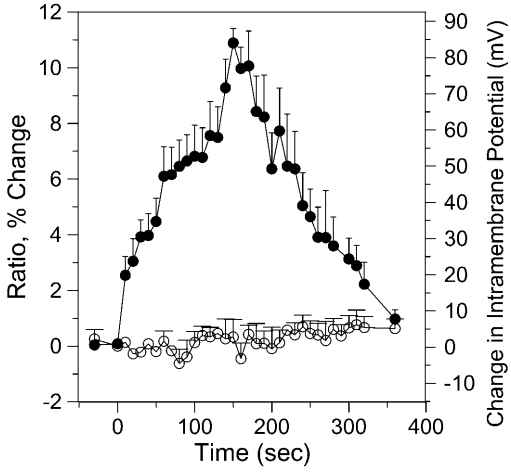

FIGURE 1 Fluorescence ratios of N1E-115 neuroblastoma cells in response to bradykinin. At time = 0, 1 μM bradykinin or EBSS was externally applied to the bathing medium of a cell stained with di-8-ANEPPS. The 440 nm/530 nm fluorescence ratios were collected with a cooled CCD camera. The relative change in ratio (*left Y axis*) and the calculated change in intramembrane potential as an equivalent of transmembrane potential (*right Y axis*) versus time were plotted. Each point is the mean ± SE of bradykinin-treated (*filled circle*, $n = 11$) or EBSS-treated cells (*empty circle*, $n = 5$).

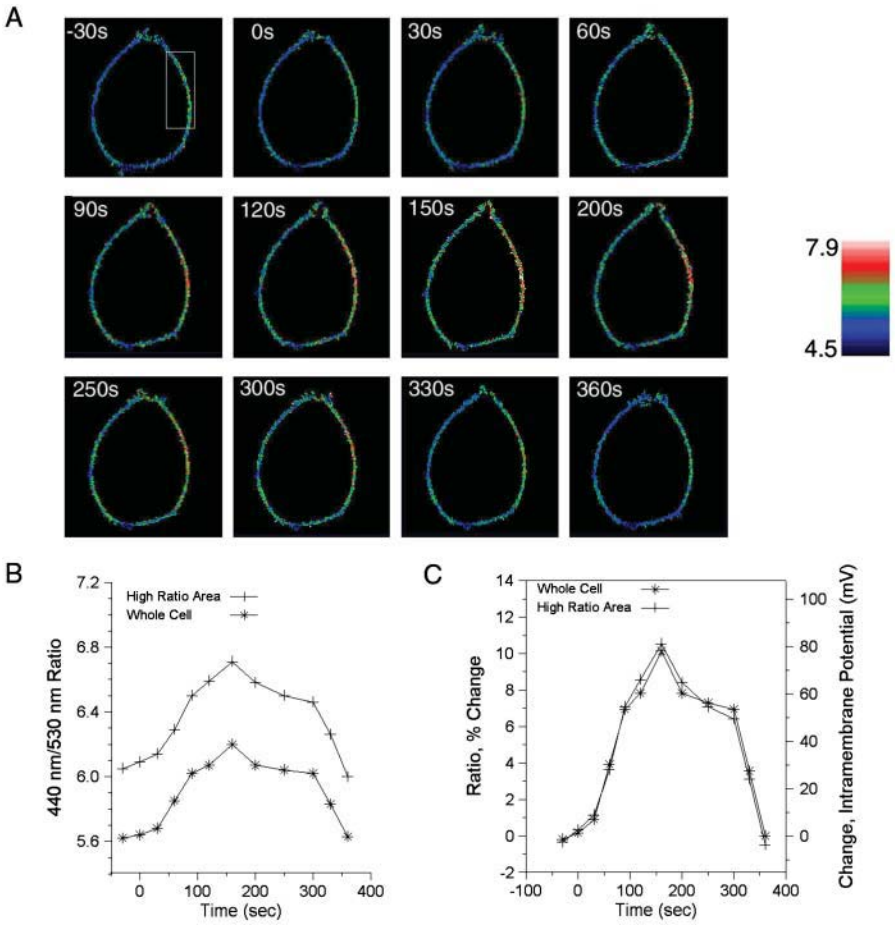

FIGURE 2 Bradykinin increases the intramembrane potential along the surface of a single N1E-115 neuroblastoma cells. (*A*) The intramembrane potential along the surface of the cell, measured by the pseudocolored 440 nm/530 nm fluorescence ratios, increases to a peak at 160 s and decays to baseline in the continued presence of bradykinin. (*B*) The 440 nm/530 nm fluorescence ratio of the whole cell (*) and of high ratio area (*framed area* in panel *A*, +) versus time. (*C*) The relative change in ratio (*left Y axis*) and the calculated change in intramembrane potential as an equivalent of transmembrane potential (*right Y axis*) for the whole cell (*) and the high ratio area (filled +) versus time.

the membrane in N1E-115 neuroblastoma cells (Tertoolen et al., 1987). To test to what extent the depolarization of transmembrane potential may contribute to the observed change in intramembrane potential, we monitored the transmembrane potential on N1E-115 cells under whole cell current clamp. Tertoolen et al. (1987) reported that addition of bradykinin (2 μM) to N1E-115 cells induced an immediate hyperpolarization (10–15 s) followed by a depolarization of the membrane (5–10 mV, lasts for a few minutes) in all the cells tested using conventional electrophysiological techniques. The transient hyperpolarization was caused by activation of $I_{K(Ca)}$ (Tertoolen et al., 1987; Higashida and Brown, 1987). $I_{K(Ca)}$ was inhibited by intracellular Mg^{2+} and could only be recorded reliably by using citrate but not acetate as the anion in the pipette, due to its high buffering capacity for intracellular Mg^{2+} (Robbins et al., 1992). In our patch-clamp experiments, 3 mM $MgCl_2$ were included and acetate was used as the anion in the pipette solution. As a result, we found that under current clamp, addition of bradykinin (1 μM) caused only a slow depolarization of the membrane potential of 7.2 $\pm$ 0.9 mV ($n = 9$) that lasted for a few minutes without apparent immediate hyperpolarization. The time to peak for bradykinin-induced depolarization ranges from 62 to 220 s (Fig. 3 *A*, panel *a* and *c*), with an average of 140.6 $\pm$ 17.6 s ($n = 9$). This is not significantly different than the time to peak for intramembrane potential modulation (158.2 $\pm$ 4.4 s; Fig. 1). The depolarization was associated with decreased conductance, as monitored by the voltage response to transient hyperpolarizing current injections (0.15 nA) (Fig. 3 *A*, panel *a*). Under voltage clamp, we recorded an M-like current in N1E-115 cells, which is characterized by slow inward relaxations during membrane hyperpolarization, (Fig. 3 *B*, panel *a*). After addition of bradykinin, these relaxations were reduced (Fig. 3 *B*, panel *b*), consistent with an inhibition of the outward current. Current-voltage curves (Fig. 3 *B*, panel *c*) showed that bradykinin inhibits a normal outward rectification current recorded at potentials positive to -60 mV, with little effect on the current recorded at potentials negative to -60 mV. These results are compatible with the view that inhibition of the voltage-dependent $I_{K(M)}$ accounts for the reduction of conductance and depolarization induced by bradykinin in N1E-115 neuroblastoma cells (Higashida and Brown, 1987). Therefore, the similar time to peak between the bradykinin-induced depolarization and intramembrane potential modulation suggests that M current inhibition and intramembrane potential modulation may be related.

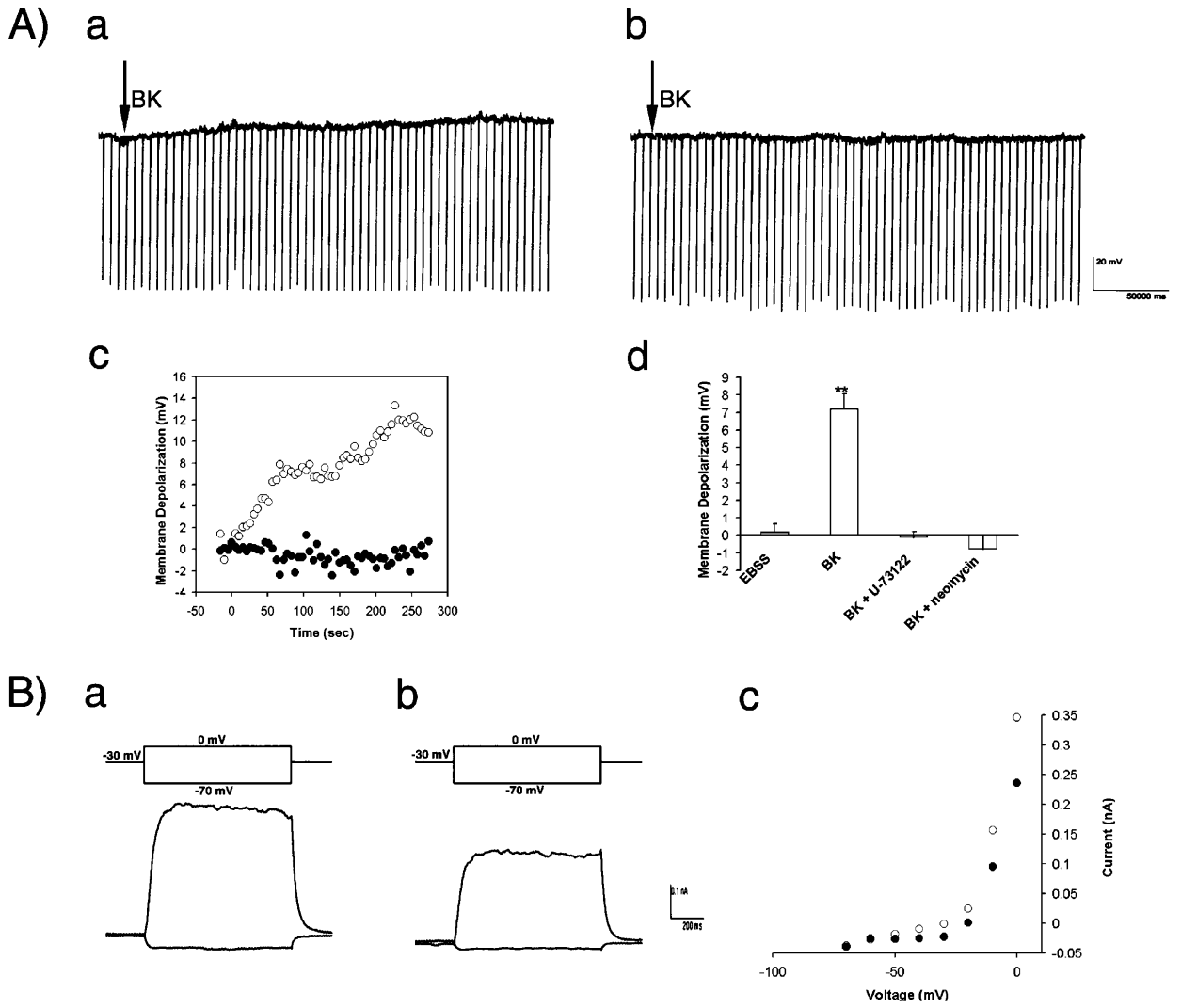

FIGURE 3 Effect of bradykinin (1 μM, added at *arrow*) on M-like current in N1E-115 neuroblastoma cell. (*A*) Membrane potential change induced by bradykinin (1 μM) in an untreated cell (panel *a*) and U-73122 pretreated cell (panel *b*). Membrane potential was recorded by whole-cell current clamp, and membrane resistance was monitored by the voltage response to brief hyperpolarizing current injections (0.15 nA). Average resting membrane potential of N1E-115 cells is -37.0 ± 2.2 mV ($n = 9$) for untreated cells, -30.7 ± 2.4 mV ($n = 8$) for U-73122 pretreated cells, and -29.2 ± 6.6 mV ($n = 5$) for neomycin. (*c*) The change in membrane potential, expressed as the measured membrane potential minus the baseline membrane potential, for the cell in panel *A*, *a* (*open circle*), and for the cell in panel *A*, *b* (*closed circle*), versus time are plotted. Bradykinin (1 μM) was added at time 0. (*d*) The PLC inhibitors blocks BK-induced membrane depolarization. Mean $\pm$ SE modulation of transmembrane potential by bradykinin (1 μM), control vehicle (EBSS) ($n = 9$), or bradykinin after pretreatment with U-73122 ($n = 8$) and neomycin ($n = 5$) are plotted. Bradykinin induced significant ($P < 0.01$, **) membrane depolarization in unpretreated cells, which was abolished by pretreatment with U-73122 and neomycin. (*B*) Leak-subtracted current responses of another voltage-clamped cell. The cell was clamped at -30 mV and stepped to -70 mV and 0 mV for 1 s before (panel *a*) and after (panel *b*) addition of bradykinin (1 μM). The graph in panel *B*, *c* shows the absolute current level attained at the end of each voltage step (ordinates, nA) plotted against the command potential (abscissae, mV) before (*open circle*) and after (*closed circle*) addition of bradykinin.

Because the peak value of bradykinin induced-depolarization of the transmembrane potential was only $\sim$7 mV, the major portion of the measured increase in intramembrane potential, namely 83mV as measured by the dye ratio, must have additional origins such as surface potential or/and dipole potential. It has been shown that N1E-115 neuroblastoma cells respond to bradykinin with an increase in $[Ca^{2+}]_i$ (Coggan and Thompson, 1995; Fink et al., 1999, 2000); an increase in $[Ca^{2+}]_i$ may also change the surface potential at the inner cell surface by screening and binding to the negative charges (McLaughlin et al., 1981). Therefore, we sought to determine whether changes in intramembrane electric potential are due to an increase in $[Ca^{2+}]_i$ by monitoring intramembrane potentials with di-8-ANEPPS and intracellular Ca^{2+} changes with Calcium Green-1-AM simultaneously.

Bradykinin raises $[Ca^{2+}]_i$ and increases intramembrane potential in the same N1E-115 cells

Consistent with the results of Fink et al (1999, 2000), we found that saturating concentrations of Bradykinin (1 μM) induced a rapid spikelike increase in $[Ca^{2+}]_i$ that decays to basal levels within 70 s of stimulation (Fig. 4). The calcium increase is observed within 6 s, with peak fluorescence increase approximating 20% (20.0 $\pm$ 2.14%, $n = 11$), occurring 8–10 s after the addition of bradykinin.

Dual wavelength ratiometric imaging of di-8-ANEPPS in the membrane and fluorescence imaging of Calcium Green in the cytosol were also performed simultaneously. Fig. 4 shows that in the eight cells that showed significant increase in $[Ca^{2+}]_i$, bradykinin raises Calcium Green fluorescence by $\sim$20% (19.8 $\pm$ 3.4%, $n = 8$) with time to peak of $\sim$10 s and a return to baseline within 70 s. However, in the same population of cells, the intramembrane potential reaches peak (11.1 $\pm$ 0.8%, $n = 8$) 150 s after the addition of bradykinin and returns to baseline within 300 s. Although the increase in intracellular calcium concentration should screen surface charge along the inner surface of the cell, thereby increasing the intramembrane potential, the distinct difference in the time course of these two effects indicates that a rise in $[Ca^{2+}]_i$ cannot be directly responsible for the dramatic increase in intramembrane potential induced by bradykinin. Furthermore, Fink et al. (1999, 2000) showed that the resting $[Ca^{2+}]_i$ in N1E-115 neuroblastoma cells is around 50 nM, and a saturating dose of bradykinin increases $[Ca^{2+}]_i$ to 1200 nM. Using the Gouy-Chapman-Stern theory elaborated by McLaughlin et al. (1981), if we assume the net negative charge density at the inner surface of the membrane is 0.14 e/nm^2 (Chandler et al., 1965), such an increase in the cytosolic Ca^{2+} concentration would cause a change in surface potential at the inner membrane surface of <0.1 mV. This is further indication that $[Ca^{2+}]_i$ cannot contribute directly to the observed change in intramembrane potential. However, it is quite possible that the calcium signal and the intramembrane potential change share portions of the same pathway.

It is noteworthy that even using saturating concentrations of BK, not all the N1E-115 cells were responsive. The calcium levels did not change in three out of 16 cells (19%) challenged with bradykinin, possibly due to inadequate receptor density. This percentage of nonresponsive cells is similar to our earlier report (Fink et al., 1999, 2000). We believe this provides a good internal control to explore whether bradykinin-induced calcium response shares the same pathway as the increase in intramembrane potential. We did find that there was a significant correlation between the calcium response amplitude and the peak intramembrane potential responses to bradykinin (Fig. 5). The linear regression analysis of the data in Fig. 5 indicates there is a significant ($P < 0.01$) direct linear correlation between the changes in intramembrane potential and $[Ca^{2+}]_i$, with a correlation coefficient (r) of 0.787. Most noteworthy, however, the three cells in Fig. 5 that did not respond to bradykinin with a strong increase in $[Ca^{2+}]_i$ also did not

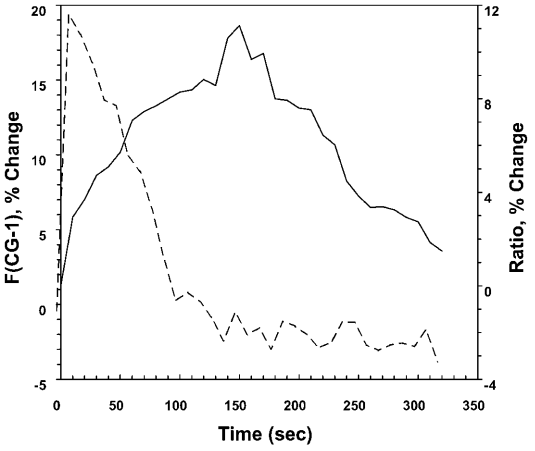

FIGURE 4 Effects of bradykinin on modulating intracellular Ca and intramembrane potentials in the responding N1E-115 cells. At time = 0, 1 μM bradykinin was externally applied to the bathing medium of the cells stained with both Calcium Green-1-AM (CG-1) and di-8-ANEPPS. Calcium Green fluorescence (*dashed curve*) and fluorescence ratios of di-8-ANEPPS (*solid curve*) recorded simultaneously were plotted versus time. Each data point represents the mean $\pm$ SE of the eight cells that showed significant response to bradykinin.

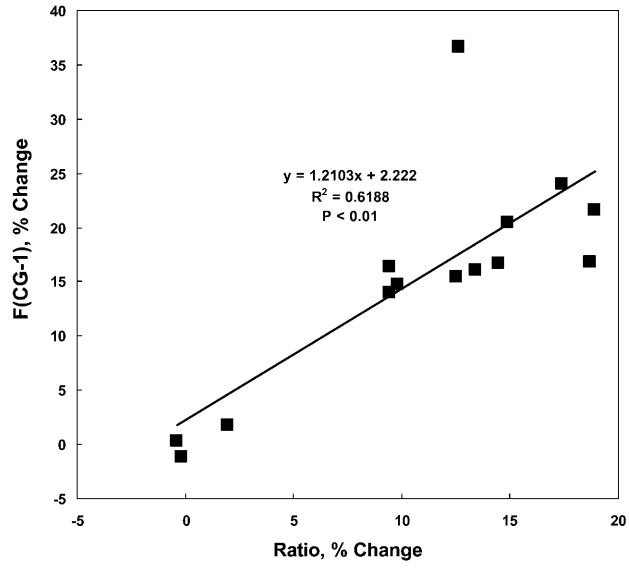

FIGURE 5 Correlation between the relative change in intramembrane potential and the increase in Calcium Green fluorescence induced by bradykinin. The relative change in Calcium Green fluorescence at 10 s was plotted versus the relative change in the 440 nm/530 nm fluorescence ratio of di-8-ANEPPS at 150 s after the addition of bradykinin (1 μM). A correlation coefficient (r) of 0.70 was obtained by correlation analysis ($P < 0.05$). Data were obtained from 14 cells that were double stained with di-8-ANEPPS and Calcium Green-1-AM and then treated with 1 μM bradykinin at time = 0.

respond with an increase in intramembrane potential. These results suggest that these two effects may share at least part of the same signal pathway. The $[Ca^{2+}]_i$ elevation in N1E-115 neuroblastoma cells in response to bradykinin is mediated by the B_2 receptor. This calcium response arises exclusively from IP_3-dependent release of calcium from endoplasmic reticulum (ER) stores, since its amplitude is not dependent upon extracellular calcium (Iredale et al., 1992; Coggan and Thompson, 1995) or the activation of ryanodine receptors in the ER (Wang and Thompson, 1995). Thus, even though the time courses are different, the close correlation between the changes in intramembrane potential and $[Ca^{2+}]_i$ suggests that the bradykinin-induced increase in intramembrane potential is probably mediated by B_2 receptors and requires activation of PLC.

PLC inhibitors block bradykinin modulation of intramembrane potential and transmembrane potential

To test whether the bradykinin-induced increase in intramembrane potential needs activation of PLC, we pretreated the N1E-115 neuroblastoma cells with two different PLC inhibitors, neomycin (500 μM) or U-73122 (1 μM). Neomycin can reduce IP_3 formation by binding to phosphoinositides (Slivka and Insel, 1988). Pretreatment with 1 μM U-73122 has been shown to block bradykinin-induced Ca^{2+} transients in dorsal root ganglion neurons and NG108-15 cells (Jin et al., 1994) and bradykinin-inhibition of $I_{K(M)}$ in dorsal root ganglion neurons (Cruzblanca et al., 1998). We also used U-73343, an inactive analog of U-73122, as a control. In our experiments, N1E-115 neuroblastoma cells were preincubated with the PLC inhibitors or EBSS solution (as control) for 30 min before the addition of bradykinin. The peak changes in intramembrane potential as measured by dye ratio after addition of bradykinin in different cell groups are summarized in Fig. 6. The bradykinin-induced increase in dye ratio (i.e., intramembrane potential) is significantly lower in cells treated with U-73122 ($1.0 \pm 0.32\%$, $n = 12$) or neomycin ($0.93 \pm 0.56\%$, $n = 8$), compared to control cells ($7.73 \pm 4.71\%$, $n = 17$) ($P < 0.01$) or cells treated with U-73343 ($4.97 \pm 1.43\%$, $n = 11$) ($P < 0.01$). There was no significant difference between bradykinin modulations of intramembrane potential in U-73343-treated neuroblastomas and control neuroblastoma cells ($P > 0.05$). The fact that the PLC inhibitors block bradykinin-induced increase in intramembrane potential, whereas the inactive U compound U-73343 has no effect, suggests bradykinin modulation of intramembrane potential involves activation of PLC.

The effect of U-73122 and neomycin on transmembrane potential is summarized in Fig. 3 *A*, panel *d*. We compared the effect of bradykinin on untreated neuroblastoma cells and PLC inhibitor-pretreated neuroblastoma cells. Before the addition of bradykinin (1 μM), there was no significant difference between resting potential in the EBSS control

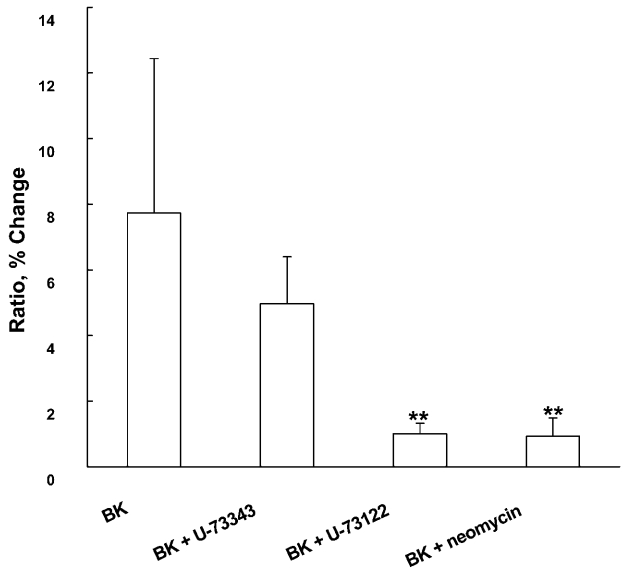

FIGURE 6 The PLC inhibitors block BK-induced increase in intramembrane potential. Mean ± SE modulation of di-8-ANEPPS fluorescence ratio and corresponding intramembrane potential by bradykinin (1 μM) in neuroblastoma cells treated with EBSS ($n = 15$), U-73343 ($n = 11$), U-73122 ($n = 10$), or neomycin ($n = 8$) is plotted. The BK-mediated increase in ratio is significantly lower in cells treated with U-73122 and neomycin than in control EBSS treated cells ($P < 0.01$, **).

group (-33.0 ± 2.0 mV, $n = 5$) versus the U-73122 group (-30.7 ± 2.4 mV, $n = 8$) and the neomycin group (-29.2 ± 6.6 mV, $n = 5$). However, the bradykinin-induced depolarization was abolished in the U-73122 group (-0.1 ± 0.3 mV, $n = 8$) or the neomycin group (-0.8 ± 0.8 mV, $n = 5$), compared to the cells treated only with bradykinin (7.2 ± 0.9 mV, $n = 9$) (Fig. 3 *B*). At the same time, the bradykinin-induced decrease in membrane conductance was abolished by pretreatment with PLC inhibitor (Fig. 3 *A*, panel *b*). Higashida and Brown (1987) have demonstrated that the bradykinin-induced decrease in conductance was due primarily to inhibition of the M current. Taken together, there is a strong parallel between the responses of $I_{K(M)}$ and the intramembrane electric field to activation of the B_2 bradykinin receptor with respect to both pharmacology and kinetics.

PIP_2 composition of N1E-115 cell membrane

The finding that PLC inhibitors blocked the bradykinin modulation of intramembrane potential suggests an involvement of hydrolysis of membrane PIP_2. To examine the relative content of PIP_2 in the cell membrane, cells were labeled to equilibrium with $^{32}P\text{-}PO_4^{2-}$. We used a thin layer chromatography system to resolve PIP_2 from the other phosphoinositides (phosphatidylinositol, phosphatidylinositol 4-phosphate) and all other plasma membrane phospholipids (Gonzalez-Sastre and Folch-Pi, 1968). The identity of

PIP_2 was also verified by cochromatographing unlabeled authentic PIP_2 standards and visualizing them with phosphomolybdic acid. Our data showed that PIP_2 comprised 0.43 ± 0.02% of total cellular phospholipids. Application of a simplified version of the Gouy-Chapman theory (McLaughlin et al., 1981, but see a more thorough analysis in the Discussion section) suggests that even if all the PIP_2, each contributing three negative charges, were depleted from the inner membrane by hydrolysis to DAG and IP_3, this could account for no more than 4 mV of the change in intramembrane potential. We therefore explored the contribution of a change in dipole potential to the overall change in intramembrane potential.

DAG increases intramembrane potential in both phosphatidylcholine and phosphatidylserine vesicles

It has been shown that the dipole potential of a DAG monolayer is significantly higher than that of a phosphatidylinositol monolayer (Smaby and Brockman, 1990). In the next experiment, we examined whether DAG could change intramembrane potential in lipid bilayers using voltage sensitive dye di-4-ANEPPS. We switched to di-4-ANEPPS for these experiments because the voltage sensitivity of this dye has been better characterized and fully calibrated in lipid vesicles (Montana et al., 1989), whereas no such prior work has been done with di-8-ANEPPS. We measured the effect of incorporating 10% DAG on the excitation spectra of di-4-ANEPPS in both PC and PS vesicles. Addition of DAG shifts the excitation spectra of di-4-ANEPPS for both lipids. The lipid-bound dye has an excitation maximum at 468 nm in PC vesicles, 466 nm in PC:DAG vesicles, 472 nm in PS vesicles, and 469 nm in PS:DAG vesicles. By normalizing the areas of the excitation spectra obtained in the presence of DAG to the integrated intensity obtained in the absence of DAG, we found that in PS vesicles, the maximum positive and negative changes in excitation spectrum induced by DAG occur at the wavelengths 440 nm and 505 nm, respectively (Fig. 7). DAG induced similar change in the excitation spectra of di-4-ANEPPS bound to PC vesicles, but of smaller amplitude (data not shown). Montana et al. (1989) found that the ratio of di-4-ANEPPS fluorescence excited at 440 and 505 nm has a linear relationship to transmembrane potential with a slope of 9%/100 mV. To determine the change in intramembrane potential induced by DAG, the ratio of fluorescence excited by these two wavelengths was recorded, and the change in intramembrane potential (ΔV_{IM}) induced by DAG was calculated as: $\Delta V_{IM} = (R - R_0)/R_0 \times 100$ mV/0.09, where R was the 440/505 nm fluorescence ratio for DAG incorporated vesicles and R_0 was the fluorescence ratio in the absence of DAG. We found the fluorescence ratios for PC, PC:DAG, PS, and PS:DAG were 1.59 ± 0.01 ($n = 3$), 1.61 ± 0.01 ($n = 6$), 1.33 ± 0.01 ($n = 11$), and 1.39 ± 0.00 ($n = 12$), respectively. Compared to pure PC vesicles, 10% DAG increased intramembrane potential of 27.2 ± 4.4 mV in PC:DAG vesicles. Compared to pure PS vesicles, 10% DAG increased intramembrane potential of 49.5 ± 2.7 mV in PS:DAG vesicles.

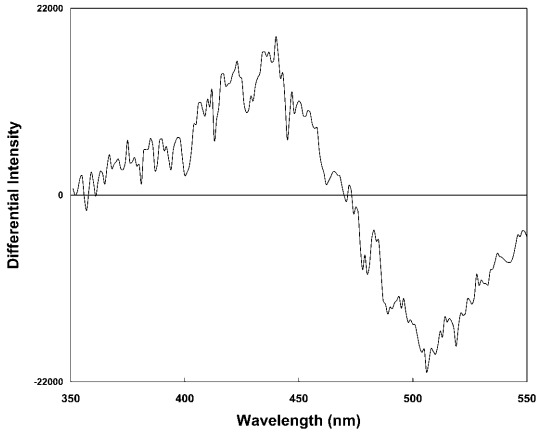

FIGURE 7 DAG induces wavelength shifts revealed by normalized difference spectra of PS lipid vesicles containing 0.2 μM di-4-ANEPPS. The plot represents the difference in the normalized excitation spectrum of pure PS vesicles and vesicles composed of 9:1 PS:DAG; the emission wavelength is 610 nm.

Parenthetically, there was also a significant difference (169.5 ± 6.2 mV) in intramembrane potential between pure PC and PS vesicles. It should be mentioned that in both PC and PS vesicles, the surface potentials at the inner and outer surfaces are symmetrical. Therefore the difference between internal and external surface potentials does not contribute to intramembrane potential, and the difference in intramembrane potential between PC and PS vesicles is due to a difference in dipole potential. Our result is consistent with the finding that the dipole potential of a PC monolayer is ~132 mV higher than that of a PS monolayer (Brockman, 1994), further validating the application of the dual wavelength fluorescence ratio for the measurement of dipole potential.

DISCUSSION

We have provided evidence that activation of PLC can dramatically change intramembrane potential and that voltage-sensitive dyes can be used to monitor these dynamic changes in single cells. Bradykinin elicited an increase in intramembrane potential in N1E-115 neuroblastoma cells by an amount equivalent to a depolarization of 83 mV. The time course for this increase in intramembrane potential is similar to the change in transmembrane potential associated with BK-mediated inhibition of $I_{K(M)}$; however, the latter increased only 7.2 ± 0.9 mV. The BK-induced release of calcium from the ER in these cells has been thoroughly studied and is known to involve, in turn, activation of PLC, hydrolysis of PIP_2 to form IP_3 and DAG, and the activation

of IP_3 receptor calcium channels in the ER. The increase in intramembrane potential is likely to also require activation of PLC, because we determined that: i), it is not found in the minor group of cells that do not display Ca^{2+} release; ii), its amplitude was significantly correlated with the amplitude of $[Ca^{2+}]_i$ elevation; and (iii), it was blocked by the PLC inhibitors U-73122 and neomycin. This Discussion will explore the possible biophysical origins of the change in intramembrane potential and its role in the modulation of $I_{K(M)}$.

The intramembrane potential is comprised of transmembrane potential, the difference between internal and external surface potential, and the internal and external dipole potential. The potential profile within the cell membrane can be derived from the sum of the potential profiles due to each of these contributions. In interpreting the dye signal, it is important to keep in mind that the ratio is fundamentally sensitive to the potential gradient (i.e., electric field) at its location rather than the actual value of potential relative to some distant arbitrary ground. First, from current-clamp measurement of membrane potential, we know that the measured 83 mV increase in intramembrane potential induced by bradykinin has only a minor contribution, 7 mV, from transmembrane depolarization. The remaining increase in intramembrane potential (~76 mV) may have significant contributions from changes in surface potential and dipole potential caused by the loss of PIP_2 and its replacement DAG. The second source of intramembrane potential is surface potential. Considering that the membrane loses ~3 negative charges for every PIP_2 that is hydrolyzed upon bradykinin-induced PLC activation, the increase in intramembrane potential may be partially explained by a decreased surface potential at the inner side of the plasma membrane. Thin layer chromatography analysis of the ^{32}P incorporation into the cellular lipids showed that PIP_2 comprised 0.43% of the total cellular phospholipids, which consist of phospholipids from both plasma membrane and intracellular membranes including endosomes, endoplasmic reticulum, lysosomes, mitochondria, nucleus, and Golgi. It has been found that ~50% of total cellular phospholipids are present in the plasma membrane of cultured cells (Warnock et al., 1993; Lange et al., 1989). Additionally, it has been found that ~40% of total cellular PIP_2 are present in the plasma membrane of cultured cells (Watt et al., 2002). Taking these factors into consideration, the basal level of PIP_2 comprises ~0.3% of phospholipids in the plasma membrane in our neuroblastoma cells. Furthermore, the percentage content of PIP_2 relative to the phospholipids in the inner leaflet of the plasma membrane would be 0.5%, since 80% of PIP_2 are found in the inner leaflet of the plasma membrane. Using the Gouy-Chapman-Stern theory (Chandler et al., 1965; Gilbert and Ehrenstein, 1969; McLaughlin et al., 1981), we can estimate the changes in surface potential at inner surface of the membrane after hydrolysis of all these PIP_2 molecules. If we assume the free negative charge density for the inner surface of the membrane is 0.14 e/nm^2 (Chandler et al., 1965), hydrolysis of such an amount of PIP_2 in the inner leaflet should lead to an increase in internal surface potential of ~4 mV (i.e., from −24 mV to −20 mV). Similarly, as described in the Results, the change in Ca^{2+} is too small to significantly screen the internal surface charge and is in any case too fast to account for the change in intramembrane potential. Therefore, the major portion of the increase in intramembrane potential cannot be attributed to obvious mechanisms for modulation of surface potential.

The third source of intramembrane potential that must be considered is the dipole potential. The dual wavelength fluorescence ratio of di-8-ANEPPS has been shown to be particularly sensitive to dipole potential because the sensor chromophore is situated just within the membrane where the electric field set up by this potential is most intense (Gross et al., 1994). Most relevant here is an earlier monolayer study showing a striking dipole potential difference between monolayers containing phosphatidylinositol and monolayers containing its PLC mediated hydrolysis product, DAG (Smaby and Brockman 1990). In this study we measured the effect of 10% DAG on intramembrane potential in PC and PS vesicles. DAG increased intramembrane potential in both PC (27 mV) and PS vesicles (49 mV). Therefore, one might expect that generation of DAG from hydrolysis of PIP_2 at the inner leaflet of the plasma membrane could produce a large increase in dipole potential. But will a dye probe that is situated on the outer leaflet of the membrane be sensitive to a dipole potential change associated with the inner leaflet? The region of largest electric field (i.e., the steepest potential gradient) associated with dipole potential occurs within a few Å of the membrane surface, so the dye ratio will be much more sensitive to a change in lipid composition in its own leaflet of the bilayer (Gross et al., 1994). This might be expected from an equilibration of DAG across the membrane because it is known to have an extraordinarily high rate of spontaneous flipping—in lipid vesicles, the time constant for DAG equilibration across the bilayer is 70 ms compared to hours for phospholipids (Bai and Pagano, 1997). Our analysis of the IP_3 production necessary to evoke the observed calcium signals after saturating bradykinin (Fink et al., 2000) indicates that newly formed DAG reaches a level of 12,560 molcules/μm^2, or ~0.9% of the internal membrane (this is similar to the initial concentration of PIP_2, but could also reflect some resynthesis of PIP_2 as a consequence of BK stimulation (Xu et al., 2003). Given that 10% DAG produces a dipole potential change of 30–40 mV in lipid vesicles, 0.9% DAG is still, therefore, insufficient to explain the observed BK-induced change in the neuroblastoma cell di-8-ANEPPS fluorescence ratio.

However, it has been reported that in both a dorsal root ganglion × neurotumor hybrid cell line F11 (Francel and Dawson, 1988) and fibroblasts (van Blitterswijk et al., 1991; Fu et al., 1992), bradykinin induces a biphasic increase in DAG, with an initial rapid, transient peak followed by a more slowly developing accumulation that increases cellular DAG

level up to three- to fourfold. The first peak is caused by PIP_2 hydrolysis and is accompanied by an increase in IP_3 and $[Ca^{2+}]_i$. The second increase reaches its peak after minutes and comes from hydrolysis of PC, by the phospholipase C that acts on PC (PC-PLC), or by the concerted action of phospholipase D (PLD) and phosphatidate phosphohydrolase (van Blitterswijk et al., 1991). The activation of PC-PLC and PLD in many cases is thought to follow the PKC activation by DAG originating from the initial hydrolysis of PIP_2 (Exton, 1994). In N1E-115 cells, therefore, activation of PLC by bradykinin could induce the subsequent activation of PC-PLC and/or PLD to generate substantial DAG in a prolonged phase, thereby producing a large change in intramembrane potential. Additional support for this scenario can be found in many published studies, e.g.:

1. It has been found that in NG108-15 cell line, bradykinin induces both generation of DAG from hydrolysis of PIP_2 (Yano et al., 1985) and a sustained increase in non-PIP_2 derived-DAG (Brami et al., 1991).
2. Bradykinin activates PLD in PC12 cells (Purkiss et al., 1991).
3. Dimethylsulfoxide induces a biphasic increase in DAG levels in N1E-115 cells (Clejan et al., 1996), with an initial rapid, transient peak followed by a slowly developing accumulation that increases cellular DAG level up to twofold; the first phase of DAG is generated through PIP_2 hydrolysis, whereas the second phase of DAG is generated through PC-PLC-mediated hydrolysis of PC. This result demonstrates that the coupling mechanism between hydrolysis of PIP_2 and activation of PC-PLC exists in N1E-115 cells.
4. There is a high basal level of DAG in N1E-115 neuroblastoma cells (1300 pmol/mg protein) (Clejan et al., 1996). Generally, neuroblastoma cells tend to have a high basal level of DAG. For example, the basal level of DAG is 2000 pmol/mg protein in NG 108-15 cells (Brami et al., 1991), 1500 pmol/mg protein in human SK-N-SH cells (Lee et al., 1991), and comprises 2.2% of cellular phospholipids in mouse NB41A3 cells (Yorek et al., 1994).

A typical differentiated N1E-115 cell used in our experiments has a diameter of 40 μm, and 400 pg protein. Assuming the molecular area of a phospholipid is 70 $Å^2$, the basal DAG would comprise ~4% of cellular lipids. If bradykinin-induced hydrolysis of PIP_2 did activate PC-PLC (or PLD) and induced subsequent increase in DAG up to threefold, that could produce an increase in DAG from ~4% to 12% of cell lipids. That could be sufficient to account for the observed increase in intramembrane potential, especially if we also consider the possibility of lipid domains that are enriched in both dye and DAG. Thus, only 15–20 mV of the observed change in intramembrane potential could arise from the measured change in transmembrane potential and the inferred changes in surface and dipole potential due to hydrolysis of PIP_2 to DAG; the remaining ~60 mV could arise from the dipole potential changes induced by the subsequent hydrolysis of PC to form DAG.

Bradykinin also produces two membrane current changes when applied to N1E-115 mouse neuroblastoma cells (Higashida and Brown, 1987), rat pheochromocytoma PC12 cells (Villarroel et al., 1989), and NG 108-15 cells (Brown and Higashida, 1988; Robbins et al., 1993). It activates a transient Ca^{2+}-dependent K^+ conductance that is associated with an increase in intracellular calcium; and it inhibits an M-type voltage-dependent K^+ current ($I_{K(M)}$) that develops more slowly and lasts for minutes. The M current ($I_{K(M)}$) is a time- and voltage-dependent K^+ current activated over the range −70 mV–0 mV. It plays an important role in regulating cell membrane excitability by stabilizing the resting membrane potential. M current inhibition by bradykinin is mediated by a pertussis toxin-insensitive G-protein (Villarroel, 1996), specifically by $G_{\alpha q}$ and/or $G_{\alpha 11}$ (Jones et al., 1995) that activates PLC.

Whereas Cruzblanca et al. (1998) showed that bradykinin used intracellular Ca^{2+} as second messenger to inhibit $I_{K(M)}$ in rat sympathetic neurons, the mechanism underlying bradykinin suppression of $I_{K(M)}$ in N1E-115 neuroblastoma cells, PC12 cells, and NG 108-15 cells remains unclear. It seems that Ca and IP_3 are not likely to be the ''messenger'', since in these cells i), inhibition of $I_{K(M)}$ persists when the release of Ca and /or activation of $I_{K(Ca)}$ is suppressed by buffering internal Ca with BAPTA (Villarroel et al., 1989); ii), inhibition of $I_{K(M)}$ is not replicated by Ca^{2+} injection (Higashida and Brown, 1986); and iii), introduction of IP_3 into the cells does not inhibit $I_{K(M)}$ nor does it block the subsequent inhibition of $I_{K(M)}$ by bradykinin, even though it does inhibit bradykinin-induced activation of $I_{K(Ca)}$ (Villarroel et al., 1989; Higashida and Brown, 1986, 1987; 1988). Our finding that the IP_3-Ca^{2+} release event has a much shorter duration and a much faster onset than M current inhibition also suggests that Ca^{2+} elevation is not likely to be directly responsible for M current modulation in N1E-115 neuroblastoma cells, although M current inhibition requires activation of PLC, since it can be blocked by PLC inhibitors U-73122 and neomycin.

The dramatic change in the electric potential profile of the lipid bilayer that occurs after hydrolysis of PIP_2 could affect the voltage-dependence of ion channels including M-type potassium channels in the membrane. In the present work, we found that bradykinin reduced the M channel conductance in a voltage-sensitive manner. In addition, bradykinin increased intramembrane potential and inhibited $I_{K(M)}$ with similar kinetics. These results are consistent with the hypothesis that an increase in intramembrane potential, possibly induced by PC-derived DAG, leads to an inhibition of $I_{K(M)}$ channels in N1E-115 cells. Indeed, it has been found that 1-oleoyl-2-acetylglycerol, a membrane-permeable DAG analog (Kaibuchi et al., 1985), mimicked bradykinin-induced inhibition of $I_{K(M)}$ (Brown and Higashida, 1988). DAG analogs also directly inhibit cloned voltage-gated

Shaker IR, Kv1.4, and Kv1.6 potassium channels (Bowlby and Levitan, 1995), cardiac L-type calcium channels (Conforti et al., 1995; Schreur and Liu, 1996), and rod cyclic nucleotide-gated channels (Gordon et al., 1995) without a PKC-dependent phosphorylation reaction. Therefore, it is possible that the increase in intramembrane potential is the underlying mechanism for M current inhibition by bradykinin in these cells.

Finally, it should be noted that an increased intramembrane potential would not necessarily affect all the ion channels that reside in the membrane to the same extent. This is because the primary contribution to the measured change in intramembrane potential likely arises from an increase in dipole potentials, which are localized to an ~5 Å thick region within the plasmalemma just below the lipid-aqueous interface. The gating sensors of different ion channels could be experiencing very different electric fields depending on whether they are located in this region.

In summary, we have shown that BK-mediated activation of PLC induces an increase in intramembrane potential in neurons. The increase in intramembrane potential has minor contributions from: a depolarized transmembrane potential; an increased surface potential at the inner surface, as the negatively charged PIP_2 is depleted; and an increased dipole potential, as PIP_2 is hydrolyzed to diacylglycerol. Its major contribution, we hypothesized, is an increased dipole potential produced by PC-derived DAG, as PC is hydrolyzed by PC-PLC or PLD after activation of PLC. This increase in intramembrane potential could be an underlying mechanism for M current inhibition by bradykinin, since the two events have similar kinetics and both can be blocked by PLC inhibitors.

We are pleased to acknowledge Jim Schaff, Dr. James Watras, and Dr. Mei-de Wei for providing advice and help in various aspects of this research.

We are grateful for the support of the National Institute of General Medical Science through grant No. GM35063.

REFERENCES

Agranoff, B. W., P. Murthy, and E. B. Seguin. 1983. Thrombin-induced phosphodiesteratic cleavage of phosphatidylinositol bisphosphate in human platelets. *J. Biol. Chem.* 258:2076–2078.

Bai, J., and R. E. Pagano. 1997. Measurement of spontaneous transfer and transbilayer movement of BODIPY-labeled lipids in lipid vesicles. *Biochemistry.* 36:8840–8848.

Bedlack, R. S., Jr., M.-d. Wei, S. H. Fox, E. Gross, and L. M. Loew. 1994. Distinct electric potentials in soma and neurite membranes. *Neuron.* 13: 1187–1193.

Berridge, M. J. 1993. Inositol trisphosphate and calcium signaling. *Nature.* 361:315–325.

Bowlby, M. R., and I. B. Levitan. 1995. Block of cloned voltage-gated potassium channels by the second messenger diacylglycerol independent of protein kinase C. *J. Neurophysiol.* 73:2221–2229.

Brami, B. A., U. Leli, and G. Hauser. 1991. Influence of lithium on second messenger accumulation in NG108-15 cells. *Biochem. Biophys. Res. Commun.* 174:606–612.

Brockman, H. 1994. Dipole potential of lipid membranes. *Chem. Phys. Lipids.* 73:57–79.

Brown, D. A., and A. Constanti. 1980. Intracellular observations on the effects of muscarinic agonists on rat sympathetic neurones. *Brit. J. Pharmacol.* 70:593–608.

Brown, D. A., and H. Higashida. 1988. Inositol 1,4,5-trisphosphate and diacylglycerol mimic bradykinin effects on mouse neuroblastoma x rat glioma hybrid cells. *J. Physiol.* 397:185–207.

Cevc, G. 1990. Membrane electrostatics. *Biochim. Biophys. Acta.* 1031: 311–382.

Chandler, W. K., A. L. Hodgkin, and H. Meves. 1965. The effect of changing the internal solution on sodium inactivation and related phenomena in giant axons. *J. Physiol. Lond.* 180:821–836.

Cladera, J., and P. O'Shea. 1998. Intramembrane molecular dipoles affect the membrane insertion and folding of a model amphiphilic peptide. *Biophys. J.* 74:2434–2442.

Clarke, R. J. 1997. Effect of lipid structure on the dipole potential of phosphatidylcholine bilayers. *Biochim. Biophys. Acta.* 1327: 269–278.

Clarke, R. J., and D. J. Kane. 1997. Optical detection of membrane dipole potential: avoidance of fluidity and dye-induced effects. *Biochim. Biophys. Acta.* 1323:223–239.

Clejan, S., R. S. Dotson, E. W. Wolf, M. P. Corb, and C. F. Ide. 1996. Morphological differentiation of N1E–115 neuroblastoma cells by dimethyl sulfoxide activation of lipid second messengers. *Exp. Cell Res.* 224:16–27.

Coggan, J. S., and S. H. Thompson. 1997. Cholinergic modulation of the Ca^{2+} response to bradykinin in neuroblastoma cells. *Am. J. Physiol.* 273:C612–C617.

Coggan, J. S., and S. H. Thompson. 1995. Intracellular calcium signals in response to bradykinin in individual neuroblastoma cells. *Am. J. Physiol.* 269:C841–C848.

Conforti, L., K. Sumii, and N. Sperelakis. 1995. Dioctanoyl-glycerol inhibits L-type calcium current in embryonic chick cardiomyocytes independent of protein kinase C activation. *J. Mol. Cell. Cardiol.* 27:1219–1224.

Constanti, A., and D. A. Brown. 1981. M currents in voltage-clamped mammalian sympathetic neurons. *Neurosci. Lett.* 24:289–294.

Cruzblanca, H., D. S. Koh, and B. Hille. 1998. Bradykinin inhibits M current via phospholipase C and Ca^{2+} release from IP_3-sensitive Ca^{2+} stores in rat sympathetic neurons. *Proc. Natl. Acad. Sci. USA.* 95:7151–7156.

Deamer, D. W., and P. S. Uster. 1983. Liposome preparation: methods and mechanisms. *In* Liposomes. M. J. Ostro, editor. Marcel Dekker, New York. 27–51.

Exton, J. H. 1994. Phosphatidylcholine breakdown and signal transduction. *Biochim. Biophys. Acta.* 1212:26–42.

Fink, C. C., B. Slepchenko, I. I. Moraru, J. Schaff, J. Watras, and L. M. Loew. 1999. Morphological control of inositol-1,4,5-trisphosphate-dependent signals. *J. Cell. Biol.* 147:929–936.

Fink, C. C., B. Slepchenko, I. I. Moraru, J. Watras, J. C. Schaff, and L. M. Loew. 2000. An image-based model of calcium waves in differentiated neuroblastoma cells. *Biophys. J.* 79:163–183.

Flewelling, R. F., and W. L. Hubbell. 1986. The membrane dipole potential in a total membrane potential model. Applications to hydrophobic ion interactions with membranes. *Biophys. J.* 49:541–552.

Francel, P., and G. Dawson. 1988. Bradykinin induces the bi-phasic production of lysophosphatidyl inositol and diacylglycerol in a dorsal root ganglion X neurotumor hybrid cell line, F-11. *Biochem. Biophys. Res. Commun.* 152:724–731.

Franklin, J. C., and D. S. Cafiso. 1993. Internal electrostatic potentials in bilayers: measuring and controlling dipole potentials in lipid vesicles. *Biophys. J.* 65:289–299.

Fu, T., Y. Okano, and Y. Nozawa. 1992. Differential pathways (phospholipase C and phospholipase D) of bradykinin-induced biphasic 1,2-diacylglycerol formation in non-transformed and K-ras-transformed

NIH-3T3 fibroblasts. Involvement of intracellular Ca^{2+} oscillations in phosphatidylcholine breakdown. *Biochem. J.* 283:347–354.

Gawrisch, K., D. Ruston, J. Zimmerberg, V. A. Parsegian, R. P. Rand, and N. Fuller. 1992. Membrane dipole potentials, hydration forces, and the ordering of water at membrane surfaces. *Biophys. J.* 63: 1213–1223.

Gilbert, D. L., and G. Ehrenstein. 1969. Effect of divalent cations on potassium conductance of squid axons: determination of surface charge. *Biophys. J.* 9:447–463.

Gonzalez-Sastre, F., and J. Folch-Pi. 1968. Thin-layer chromatography of the phosphoinositides. *J. Lipid Res.* 9:532–533.

Gordon, S. E., J. Downing-Park, B. Tam, and A. L. Zimmerman. 1995. Diacylglycerol analogs inhibit the rod cGMP-gated channel by a phosphorylation-independent mechanism. *Biophys. J.* 69:409–417.

Gross, E., R. S. Bedlack, and L. M. Loew. 1994. Dual-wavelength ratiometric measurement of the membrane dipole potential. *Biophys. J.* 67: 208–216.

Higashida, H., and D. A. Brown. 1986. Two ployphosphoinositide metabolites control two K^+ currents in a neuronal cell. *Nature.* 323: 333–335.

Higashida, H., and D. A. Brown. 1987. Bradykinin inhibits potassium (M) currents in N1E–115 neuroblastoma cells. Responses resemble those in NG108-15 neuroblastoma x glioma hybrid cells. *FEBS Lett.* 220: 302–306.

Higashida, H., and D. A. Brown. 1988. Ca^{2+}-dependent K^+ channels in neuroblastoma hybrid cells activated by intracellular inositol trisphosphate and extracellular bradykinin. *FEBS Lett.* 238:395–400.

Honig, B. H., W. L. Hubbell, and R. F. Flewelling. 1986. Electrostatic interactions in membranes and proteins. *Ann. Rev. Biophys. Chem.* 15:163–193.

Iredale, P., K. Martin, S. Hill, and D. Kendall. 1992. Agonist-induced changes in $[Ca^{2+}]_i$ in N1E–115 cells: differential effects of bradykinin and carbachol. *Eur. J. Pharmacol.* 226:163–168.

Jin, W., T. M. Lo, H. H. Loh, and S. A. Thayer. 1994. U73122 inhibits phospholipase C-dependent calcium mobilization in neuronal cells. *Brain Res.* 642:237–243.

Jones, S., D. A. Brown, G. Milligan, E. Willer, N. J. Buckley, and M. P. Caulfield. 1995. Bradykinin excites rat sympathetic neurons by inhibition of M current through a mechanism involving B_2 receptors and G alpha q/11. *Neuron.* 14:399–405.

Kaibuchi, K., Y. Takai, and Y. Nishizuka. 1985. Protein kinase C and calcium ion in mitogenic response of macrophage-depleted human peripheral lymphocytes. *J. Biol. Chem.* 260:1366–1369.

Kleinig, H. 1970. Nuclear membranes from mammalian liver. II. Lipid composition. *J. Cell Biol.* 46:396–402.

Lange, Y., M. H. Swaisgood, B. V. Ramos, and T. L. Steck. 1989. Plasma membranes contain half the phospholipid and 90% of the cholesterol and sphingomyelin in cultured human fibroblasts. *J. Biol. Chem.* 264: 3786–3793.

Langner, M., D. Cafiso, S. Marcelja, and S. McLaughlin. 1990. Electrostatics of phosphoinositide bilayer membranes. Theoretical and experimental results. *Biophys. J.* 57:335–349.

Lee, C., S. K. Fisher, B. W. Agranoff, and A. K. Hajra. 1991. Quantitative analysis of molecular species of diacylglycerol and phosphatidate formed upon muscarinic receptor activation of human SK-N-SH neuroblastoma cells. *J. Biol. Chem.* 266:22837–22846.

Lee, S. B., and S. G. Rhee. 1995. Significance of PIP_2 hydrolysis and regulation of phospholipase C isozymes. *Curr. Opin. Cell. Biol.* 7: 183–189.

Locher, R., L. Neyses, M. Stimpel, B. Kuffer, and W. Vetter. 1984. The cholesterol content of the human erythrocyte influences calcium influx through the channel. *Biochem. Biophys. Res. Commun.* 124:822–828.

Loew, L. M. 1993. The electrical properties of membranes. *In* Biomembranes. Physical Aspects. M. Shinitzky, editor. VCH Publishers, Weinheim, Germany. 341–371.

McLaughlin, S. 1977. Electrostatic potentials at membrane-solution interfaces. *In* Current Topics Membranes and Transport. F. Bronner and J. Kleinzeller, editors. Academic Press, New York. 71–144.

McLaughlin, S. 1989. The electrostatic properties of membranes. *Annu. Rev. Biophys. Biophys. Chem.* 18:113–136.

McLaughlin, S., N. Mulrine, T. Gresalfi, G. Vaio, and A. McLaughlin. 1981. Adsorption of divalent cations to bilayer membranes containing phosphatidylserine. *J. Gen. Physiol.* 77:445–473.

Montana, V., D. L. Farkas, and L. M. Loew. 1989. Dual-wavelength ratiometric fluorescence measurements of membrane potential. *Biochemistry.* 28:4536–4539.

Purkiss, J., R. A. Murrin, P. J. Owen, and M. R. Boarder. 1991. Lack of phospholipase D activity in chromaffin cells: bradykinin-stimulated phosphatidic acid formation involves phospholipase C in chromaffin cells but phospholipase D in PC12 cells. *J. Neurochem.* 57:1084–1087.

Robbins, J., R. Cloues, and D. A. Brown. 1992. Intracellular Mg^{2+} inhibits the IP_3-activated IK(Ca) in NG108-15 cells. (Why intracellular citrate can be useful for recording IK(Ca)). *Pflugers. Arch.* 420:347–353.

Robbins, J., S. J. Marsh, and D. A. Brown. 1993. On the mechanism of M-current inhibition by muscarinic m1 receptor in DNA-transfected rodent neuroblastoma x glioma cells. *J. Physiol.* 469:153–178.

Schreur, K. D., and S. Liu. 1996. 1,2-Dioctanoyl-sn-glycerol depresses cardiac L-type Ca^{2+} current: independent of protein kinase C activation. *Am. J. Physiol.* 270:C655–C662.

Sen, L., R. A. Bialecki, E. Smith, T. W. Smith, and W. S. Colucci. 1992. Cholesterol increases the L-type voltage-sensitive calcium channel current in arterial smooth muscle cells. *Circ. Res.* 71:1008–1014.

Slivka, S. R., and P. A. Insel. 1988. Phorbol ester and neomycin dissociate bradykinin receptor-mediated arachidonic acid release and polyphosphoinositide hydrolysis in Madin-Darby canine kidney cells. *J. Biol. Chem.* 263:14640–14647.

Smaby, J. M., and H. L. Brockman. 1990. Surface dipole moments of lipids at the argon-water interface. Similarities among glycerol-ester-based lipids. *Biophys. J.* 58:195–204.

Strichartz, G. R., G. S. Oxford, and F. Ramon. 1980. Effects of the dipolar form of phloretin on potassium conductance in squid giant axon. *Biophys. J.* 31:229–246.

Szabo, G. 1974. Dual mechanism for the action of cholesterol on membrane permeability. *Nature.* 252:47–49.

Szabo, G. 1977. Electrical characteristics of ion transport in lipid bilayer membranes. *Ann. N. Y. Acad. Sci.* 303:266–280.

Tertoolen, L. G., B. C. Tilly, R. F. Irvine, and W. H. Moolenaar. 1987. Electrophysiological responses to bradykinin and microinjected inositol polyphosphates in neuroblastoma cells. Possible role of inositol 1,3,4-trisphosphate in altering membrane potential. *FEBS Lett.* 214:365–369.

Tran, D., P. Gascard, B. Berthon, K. Fukami, T. Takenawa, F. Giraud, and M. Claret. 1993. Cellular distribution of polyphosphoinositides in rat hepatocytes. *Cell Signal.* 5:565–581.

van Blitterswijk, W. J., H. Hilkmann, J. de Widt, and R. L. van der Bend. 1991. Phospholipid metabolism in bradykinin-stimulated human fibroblasts. I. Biphasic formation of diacylglycerol from phosphatidylinositol and phosphatidylcholine, controlled by protein kinase C. *J. Biol. Chem.* 266:10337–10343.

Villarroel, A. 1996. M-current suppression in PC12 cells by bradykinin is mediated by a pertussis toxin-insensitive G-protein and modulated by intracellular calcium. *Brain Res.* 740:227–33.

Villarroel, A., N. V. Marrion, H. Lopez, and P. R. Adams. 1989. Bradykinin inhibits a potassium M-like current in rat pheochromocytoma PC 12 cells. *FEBS Lett.* 255:42–46.

Wang, S. S., and S. H. Thompson. 1995. Local positive feedback by calcium in the propagation of intracellular calcium waves. *Biophys. J.* 69:1683–1697.

Warnock, D. E., C. Roberts, M. S. Lutz, W. A. Blackburn, W. W. Young, Jr., and J. U. Baenziger. 1993. Determination of plasma membrane lipid mass and composition in cultured Chinese hamster ovary cells using

high gradient magnetic affinity chromatography. *J. Biol. Chem.* 268: 10145–10153.

Watt, S. A., G. Kular, I. N. Fleming, C. P. Downes, and J. M. Lucocq. 2002. Subcellular localization of phosphatidylinositol 4,5-bisphosphate using the pleckstrin homology domain of phospholipase C delta1. *Biochem. J.* 363:657–666.

Xu, C., and L. M. Loew. 2003. The effect of asymmetric surface potentials on the intramembrane electric field measured with voltage-sensitive dyes. *Biophys. J.* 84:2768–2780.

Xu, C., J. Watras, and L. M. Loew. 2003. Kinetic analysis of receptor–activated phosphoinositide turnover. *J. Cell Biol.* In Press.

Yano, K., H. Higashida, H. Hattori, and Y. Nozawa. 1985. Bradykinin-induced transient accumulation of inositol trisphosphate in neuron-like cell line NG108-15 cells. *FEBS Lett.* 181:403–406.

Yorek, M. A., J. A. Dunlap, M. R. Stefani, E. P. Davidson, X. Zhu, and J. Eichberg. 1994. Decreased myo-inositol uptake is associated with reduced bradykinin-stimulated phosphatidylinositol synthesis and diacylglycerol content in cultured neuroblastoma cells exposed to L-fucose. *J. Neurochem.* 62:147–158.

Zhang, J., L. M. Loew, and R. M. Davidson. 1996. Faster voltage-dependent activation of Na^+ channels in growth cones versus somata of neuroblastoma N1E-115 cells. *Biophys. J.* 71:2501–2508.

Zhang, J., M. D. Robert, M. Wei, and L. M. Loew. 1998. Membrane electric properties by combined patch clamp and fluorescence ratio imaging in single neurons. *Biophys. J.* 74:48–53.

Zheng, C., and G. Vanderkooi. 1992. Molecular origin of the internal dipole potential in lipid bilayers: calculation of the electrostaic potential. *Biophys. J.* 63:935–941.

Zhou, Q., S. Jimi, T. L. Smith, and F. A. Kummerow. 1991. The effect of cholesterol on the accumulation of intracellular calcium. *Biochim. Biophys. Acta.* 1085:1–6.